Published in final edited form as:
*Heart Rhythm*. 2009 December ; 6(12): 1782–1789. doi:10.1016/j.hrthm.2009.08.023.

# Arrhythmogenic mechanisms of the Purkinje system during electric shocks: A modeling study

**Makarand Deo, PhD**[*], **Patrick Boyle**[*], **Gernot Plank, PhD**[†], and **Edward Vigmond, PhD**[*]

[*]Department of Electrical and Computer Engineering, University of Calgary, Calgary, Canada

[†]Institute of Biophysics, Medical University of Graz, Graz, Austria

## Abstract

**Background—**The function of the Purkinje system (PS) is to ensure fast and uniform activation of the heart. Although this vital role during sinus rhythm is well understood, this is not the case when shocks are applied to the heart, especially in the case of failed defibrillation. The PS activates differently from the myocardium, has different electrophysiological properties, and provides alternate propagation pathways; thus, there are many ways in which it can contribute to postshock behavior.

**Objective—**The purpose of this study was to elucidate the role of the PS in the initiation and maintenance of postshock arrhythmias.

**Methods—**A computer model of the ventricles including the PS was subjected to different reentry induction protocols.

**Results—**The PS facilitated reentry induction at relatively weaker shocks. Disconnecting the PS from the ventricles during the post-shock interval revealed that the PS helps stabilize early-stage reentry by providing focal breakthroughs. During later stages, the PS contributed to reentry by leading to higher frequency rotors. The PS also promoted wave front splitting during reentry due to electrotonic coupling, which prolongs action potential durations at PS-myocyte junctions. The presence of a PS results in the anchoring of reentrant activations that propagate through the pathways provided by the PS.

**Conclusions—**The PS is proarrhythmic in that it provides pathways that prolong activity, and it plays a supplementary role in maintaining the later stages of reentry (>800 ms).

### Keywords

Purkinje system; Shock-induced arrhythmia; Cardiac modeling; Reentry mechanisms

## Introduction

The Purkinje system (PS) is specialized tissue responsible for the rapid, widespread distribution of electrical pulses throughout the ventricles. While the vital importance of the

**Address reprint requests and correspondence:** Dr. Makarand Deo, Ph.D., University of Michigan Ann Arbor, 5025 Venture Drive, Ann Arbor, Michigan 48108. mdeo@ucalgary.ca.


Europe PMC Funders Author Manuscripts

PS under physiological conditions is well understood, its role in postshock arrhythmogenesis remains largely unelucidated since simultaneous recording of PS and organ-level ventricular activity is experimentally difficult to achieve. The PS may affect the establishment of reentry in two ways: First, it may lead to more shock-induced myocardial excitation since shock effects in the PS are more pronounced1 owing to its one-dimensional nature and unique electrophysiology. Second, the PS may provide additional pathways for electrical activity, providing alternative routes for otherwise blocked reentrant wave fronts.2 Conversely, additional pathways may contribute to termination of reentry due to wave front annihilation and consumption of the postshock excitable gap.3 Shock effects, including selective disruption of the PS due to electroporation and sustained depolarization, are both proarrhythmic and antiarrhythmic.4

Ample evidence points to PS involvement in arrhythmogenesis. The PS contributes to ventricular fibrillaton (VF) maintenance in dogs and swine5,6 through continuous and repetitive wave breaks.7,8 Chemical PS ablation slowed activation rates and caused early termination of VF in dogs.9 Further evidence comes from catheter ablation of areas dense with Purkinje cells, which results in reduced inducibility.5 Subthreshold PS stimulation in intact guinea pig hearts interrupts ventricular tachycardia (VT) by affecting Purkinje-myocardial coupling.10 Although these studies suggest PS involvement in VT/VF, experimental limitations have prevented direct confirmation that the PS has arrhythmogenic mechanisms.

Owing to its distinct electrical, geometrical, and topological properties, the shock-induced response of the PS is quite different from that of the ventricular mass. Consequently, we hypothesize that the PS plays a pivotal role during the onset and early phase of postshock electrical activity. Using a geometrically realistic computer model of the rabbit ventricles with a topologically realistic PS, we systematically studied the role of the PS during the onset and maintenance of arrhythmias. We mimicked experimental procedures to induce reentry, teasing out PS effects by repeating each protocol with and without the PS. To assess PS contributions to postshock events, the PS was decoupled at various instants and outcomes were compared against control cases for which the PS remained intact.

## Methods

### Governing equations

Cardiac electrical activity was described by the bidomain representation of cardiac tissue.11 This formulation accounts for both intra- and extracellular potential fields ($\varphi_i$ and $\varphi_e$, respectively), which are linked by the transmembrane current density ($I_m$). Ion dynamics for the myocardium were described by the rabbit ventricular action potential model developed by Mahajan et al.12 The model was modified to include an electroporation channel13 and an outward current activated upon strong shock-induced depolarization ($I_a$).14 Numerical method details are given by Vigmond et al.11

## Modeling ventricles and conduction system

Computer simulations were performed on a tetrahedral finite element model of the ventricles, based on the San Diego rabbit heart,15 consisting of 547,680 myocardial nodes (862,515 nodes including bath and blood cavities), with an average internodal spacing of 250 $\mu$m, which is sufficient for convergence of propagation. A branching PS was implemented, as described elsewhere.16 PS endpoints were inserted into the myocardium up to one-third of the wall thickness.17 The angle of insertion was kept between 30° and 45°, with the surface tangent to avoid sharp discontinuities. Purkinje-myocardial junctions (PMJs) were modeled using fixed resistance connections to adjacent myocardial cells within a user-specified radius (average number of 56 cells). The DiFrancesco-Noble model of the Purkinje cell,18 modified to include an electroporation channel13 and an $I_a$ current component,14 characterized the ionic behavior of the PS.

Sodium conductance, tissue conductivities, gap junction resistances, and PMJ resistances were adjusted to correctly reproduce normal ventricular activation patterns recorded during sinus rhythm19 (Figure 1). PS junctional parameters were tuned to obtain realistic transmission characteristics,20 with retrograde propagation delays being much shorter (≈0.96 ms; Figure 1D) than anterograde delays (≈9.69 ms; Figure 1C).

## Reentry induction protocols

Electrode configuration and pacing protocol followed a procedure used in experimental studies of shock-induced arrhythmias.21 Reentry was induced in quiescent ventricles either by a single cross shock delivered at a variable coupling interval (CI) after transmembrane current pacing (either at the apex (AP) or at the His bundle) or by burst pacing with a pair of consecutive cross shocks separated by a variable basic cycle length (BCL). The assembly shown in Figure 1 was immersed in a bath (3 × 3 × 3 cm). In all cases, shocks were delivered by applying a uniform electric field via two plate electrodes at bath boundaries, 0.5 mm from the epicardium, in an anterior-posterior configuration. The anterior plate electrode served as a cathode, and the posterior electrode was grounded. Cross shocks were monophasic, and field strengths varied between 3 and 8.9 V/cm. Although various shock durations between 3 and 10 ms were tested during the setup phase of the study, 3-ms shocks were sufficient for inducing arrhythmias and were the most computationally efficient. Apical pacing and burst pacing were performed with the PS (AP+PS, BP+PS) and without the PS (AP−PS, BP−PS), with either CI or BCL varying between 100 and 200 ms by steps of 10 ms.

Tachyarrhythmias were considered sustained if shock-induced reentry lasted for at least 800 ms. Rotor frequencies were determined by taking the inverse of the average cycle length measured over six successive depolarizations at points chosen near, but not in, the rotor core. Phase singularities were detected using the method described by Hillebrenner et al,22 which allowed for analysis of filaments with respect to the PS.

## Results

### PS contributions to arrhythmia induction

Table 1 shows the minimum shock strengths and range of CIs for which reentry occurred in each protocol. With the PS, reentry was induced by weaker shocks than in its absence. The CI/BCL range for AP+PS and BP+PS was similar to that of AP−PS and BP−PS, respectively. Reentry was induced at the shortest intervals during burst pacing, followed by longer CIs for apical pacing and the longest intervals for His pacing.

Reentry was successfully induced with all protocols but with differences in activation patterns and complexity. Figure 2 shows Vm maps during reentry induced by BP+PS. The earliest propagated postshock activation on the epicardium was a focal breakthrough. As seen in Figure 2B, the first postshock endocardial activations always emanated from PS strands with no other activations on the epicardium. Frequently, these postshock activations degraded into figure-of-eight reentry (Figure 2D). During early postshock reentry, both reentrant and focal activity (Figure 2C and 2E) were observed on the epicardium; during later stages, activation patterns were purely reentrant, with no signs of focal activity.

Compared with BP+PS, reentry from a cross shock after single-site pacing (AP+PS and His) was more complex. Typically, figure-of-eight reentry was observed. Reentry was composed of more than one stable rotor and a large number of epicardial focal breakthrough sites. In later stages (>1000 ms), however, only one transmural filament (the I type) survived.

During simulations without PS (AP−PS and BP−PS), reentry was initiated on the free walls and in the later stages stabilized around the apex (not shown). Similar behavior was observed during shocks applied to fibrillating hearts (n = 6). The first postshock activations on endocardium and epicardium were induced by the PS during failed defibrillation shocks (5.5 and 11 V/cm).

### PS contributions to maintenance of reentry

The PS was active throughout reentry in all protocols and exhibited both anterograde and retrograde conduction at PMJs. PS activity contributed to reentry dynamics in three ways (see Figure 3). First, PS endpoints conducted intramural activity retrogradely, exciting distant endocardium ahead of the wave front, effectively accelerating propagation when the original wave front merged with the new; second, retrograde activity provided an escape route for wave fronts terminating owing to refractory tissue, thereby prolonging activity; third, refractory regions surrounding PS entry points caused fractionation in wave fronts. Since PS cells have a longer intrinsic action potential duration (APD), this sort of wave front splitting occurred frequently.

To assess the contribution of the PS to maintenance and stabilization of reentry during different phases, the PS was disconnected at various postshock instants (Figure 4). Initially, PS isolation extinguished activity. PS disconnection at 200 ms led to reentry termination at 555 ms for AP+PS, as shown in detail in Figure 5. and at 650 ms for His pacing. In contrast, PS disconnection at later stages (≥1000 ms for AP+PS and ≥750 ms for His pacing) did not

Europe PMC Funders Author Manuscripts

terminate reentry. Thus, once meandering wave fronts on the epicardium and the endocardium converged into stable rotors, the PS did not appear to play a direct role.

Figure 5 shows a breakthrough at 370 ms (see panel A) provided by the PS (seen in panel B), which induced a new wave front that helped to maintain the tachycardia. When the PS was virtually isolated at 200 ms, the breakthrough was not provided (see panel C), and as a result, the existing reentrant activations died at 462 ms (see panel F). Panels D and F show subsequent snapshots at 500 and 440 ms, in respective cases.

Nonetheless, analysis of epicardial rotors after 1000 ms (see Figure 6) revealed that rotor frequency was higher with a PS (≈8.8 Hz) than without (≈7.3 Hz). Furthermore, PS involvement mediated the location of rotor stabilization, with AP+PS rotors located on the right ventricular (RV) free wall compared with AP−PS rotors, which stabilized in the apical region.

## Breakthroughs during reentry

The number of epicardial breakthroughs was examined during various stages of reentry for AP+PS, His, and BP+PS. Figure 7 shows the average number of focal breakthroughs observed during reentry. The number of breakthroughs observed was considerably higher during early stages (0–600 ms). Most of these breakthroughs were provided by the PS, which initiated wave fronts when existing activations extinguished. These also merged with existing wave fronts. Once reentry was established, fewer breakthroughs were observed, with many being masked by reentrant myocardial activations. For apical pacing in the absence of PS, breakthroughs were reduced by approximately 50%. We further verified that the breakthroughs came from the PS by increasing the penetration depth so that the PMJs were on the epicardium (see Figure 7C). Under these conditions, the number of observed breakthroughs approximately doubled owing to the fact that there was less time for wave fronts traveling across the myocardium to merge with those emanating from PS endpoints, which resulted in fewer obscured breakthroughs.

## Phase singularities anchored to PS

Figure 8 shows phase singularities induced after His pacing at various instants. These were consistently located in regions surrounding the distal fan out of the PS, as shown in panel A. Epicardial singularities were predominantly connected to endocardial singularities by transmural I-shaped filaments, which were usually anchored around PS endpoints, as shown during the early stages of reentry in panel B. In panel D, four of five filaments are anchored to PS endpoints, with three being I-shaped (epicardial endpoints are visible in panel C) and one being U-shaped. Similarly, panels E and F show an instant with one I-shaped and two U-shaped filaments anchored around PS.

## Defibrillation

A subset of simulations was conducted by applying shocks to sustained reentry at three different CIs for AP+PS and AP−PS. For AP+PS, an 8 V/cm shock terminated activity, while for AP−PS, it did not. The most obvious difference in defibrillation response between AP+PS and AP−PS was that a PS led to much more rapid and widespread epicardial

depolarization, quickly consuming any excitable gaps. Without a PS, a larger and longer lasting excitable gap existed under the anode, allowing rotor formation. Figure 7D shows that the number of breakthroughs during the first 400 ms after failed 4 V/cm defibrillation shocks was higher with a PS.

## Discussion

This paper presents direct evidence of active PS involvement in shock-induced arrhythmogenesis and maintenance through a detailed computer simulation study. Its principal findings are that (1) the PS facilitates reentry induction at weaker shock strengths; (2) the PS stabilizes reentry during initial stages by providing focal breakthroughs; (3) with a PS, reentry was anchored in the RV and had a higher frequency; (4) the PS facilitates splitting in wave fronts that collide with regions surrounding refractory PS endpoints; (5) phase singularities were concentrated in the distal PS network with the reentrant filaments anchored to PS endpoints; and (6) the PS led to more rapid activation, which helped defibrillation. These findings are applicable to all tested protocols for reentry induction. Observations that agree with experimental findings include the following: (1) higher strength shocks produced an isoelectric window, and initial postshock focal activations degenerated into reentry23; (2) the earliest postshock activations originated in the subendocardial region24; (3) reentry was initially driven by a large number of focal breakthroughs25; and (4) later stage reentry was maintained by stable rotors and wave breaks26 with no apparent PS involvement.10 This study proposes conclusive mechanisms for these disparate experimental observations and provides novel insights regarding PS contributions to shock-induced arrhythmogenesis.

### PS favors reentry induction

Reentry induction data (Table 1) show that the PS helped induce reentry for weaker shocks. The range of CIs for AP−PS were similar to those reported in previous studies,27 barring specific distinctions pertaining to the choice of modeling parameters. The PS provided fast-conducting pathways for reentrant wave fronts before they encountered refractory myocardial tissue. PMJ retrograde conduction is favorable to anterograde conduction because of myocardial loading.28 Electrotonic interactions at PMJs shorten the refractory period in the distal PS,2 but proximal PS branches remain refractory. In such cases, retrograde conduction into the proximal PS was not possible but could still successfully activate neighboring PMJs. Therefore, wave fronts encountering resting PMJs could enter the distal PS retrogradely and activate distant excitable regions by anterograde conduction. In cases in which such activation pathways excited myocardial regions that had recently conducted the same wave front and were reexcitable, this initiated reentry.

We did not observe notable differences in PS behavior with varying shock polarity and electrode configurations (left atrial-right atrial, anterior-posterior, and apical-base). Shock-induced PS excitations were observed in branches making sharp angles with respect to the applied field, which conducted to the rest of the PS and myocardium. Since the PS has strands orientated in all directions, it exhibits similar effects for any field direction (electrode configuration).16




Europe PMC Funders Author Manuscripts

Europe PMC Funders Author Manuscripts

Scroll waves were anchored around I-shaped filaments, most of which were short-lived. Initially, reentry consisted of a large number of epicardial breakthroughs located near PS insertion points. The PS contribution to these breakthroughs was evident from the presence of PS action potentials before myocardial activation (Figure 5D). Moreover, the number of breakthroughs during initial stages of reentry increased significantly when the PMJs were brought closer to the epicardial surface. Our observations regarding focal activations during reentry induction agree with experimental findings.23,25

### PS stabilizes reentry

Reentry in the presence of a PS must adapt to the network dynamics. When excitation passes over a recovered PMJ, retrograde conduction can race through the PS, causing a breakthrough ahead of the slower propagating myocardial wave front, leading to effective acceleration. The reentry path is also adjusted until breakthroughs are no longer seen, which suggests the direct influence of the PS on the organization of arrhythmias. At this point, the PS is no longer needed but has established a stable reentry based on local propagation through the PS. Furthermore, network topology will also dictate regions about which rotors will anchor, which seemed to be the free wall for this particular shock configuration. Without a PS, reentry drifted toward the apex, where it was anchored by the conical geometry and fiber architecture. On a related note, rotor frequency was higher for simulations with the PS.

While another group previously suggested that the PS becomes less important in maintaining reentry over time,2 our study did not observe that study's report of drifting breakthroughs during reentry. This may be due to the drastically different reentry initiation methods or the more realistic model used here. Furthermore, careful analysis of breakthroughs in our results reveals that they were provided by the PS. Finally, we compared our results of reentry with and without PS to further identify the precise role of the PS.

Although the PS appeared to be irrelevant at later stages of reentry, it contributed indirectly to its maintenance. Experimentally, it was found that disruption of the PS terminated tachycardia, although the PS did not play an apparent role in conduction.10 Four major mechanisms of the PS during reentry were identified: (1) accelerating propagation by providing fast pathways; (2) providing an escape route for extinguishing wave fronts; (3) generating secondary wave fronts through wave front splitting; and (4) providing a substrate to anchor reentrant filaments. APD prolongation in regions surrounding PS insertion points led to prolongation of refractoriness due to electrotonic interactions between the coupled cells.29 This led to fractionation through wave front splitting.

### Implications for improving defibrillation efficacy

The PS appears to play both anti- and proarrhythmic roles. Excitation of the PS leads to the rapid consumption of postshock excitable gaps before reentry can form; however, if wave fronts do survive, the PS may then help reinitiate reentry. In support, Al-Khadra et al4 applied preconditioning shocks to electroporate and temporarily incapacitate the bundles and PS, demonstrating that such prior shocks reduce vulnerability to shock-provoked arrhythmias. Recently, Tang et al30 found that pacing near the site of earliest postshock

activation terminated shock-induced VF and increased defibrillation efficacy. If we consider the possibility of PS involvement during shock-induced arrhythmogenesis, such synchronized postshock pacing could have prevented PS from taking part in any reentry circuits, thus avoiding its initiation. Hence, this study will be useful in designing newer and more efficient defibrillation strategies that specifically target the PS. Furthermore, because of how the PS organizes reentry, certain reentry patterns may be more probable than others. Knowledge of such pathways may be useful when deciding where to perform ablation to treat VT.

## Limitations

Our PS structure is based on anatomical and physiological descriptions from the literature and not on a specific specimen. However, LacZ staining in adult mouse hearts has revealed that its structure is much more dense and fine.31 The structure of PMJs and the insertion of PS endpoints into the myocardium are matters of ongoing investigation. Our approach is to approximate PMJs with simple resistances and ensure proper delays and loading.

We did not apply shocks strong enough to cause electroporation (>25 V/cm). While such fields are generated in the immediate vicinity of electrodes, they are not present in the bulk myocardium. The addition of this factor would have led to additional complexity when analyzing results and will be the subject of further study. In this paper, we have presented limited results pertaining to defibrillation. Fully elucidating the role of PS during defibrillation will require a more thorough study.

## Conclusions

This paper underlines the vital role of PS in initiation and maintenance of shock-induced arrhythmias. The PS facilitated reentry induction at relatively weak shocks. The earliest postshock activations emanated from the PS, which soon degraded into reentrant activity in the case of shocks applied during the vulnerable period. The PS assisted stabilization of the rotors during the early stages of reentry and appeared to play a supplementary role by providing pathways during later stages. This study is useful in understanding the exact role of the PS in shock-induced arrhythmias and in the design of more efficient defibrillation strategies by identifying the role the PS plays in failed shocks.

Europe PMC Funders Author Manuscripts

## Acknowledgments

This research was supported by the Natural Sciences and Engineering Research Council of Canada and the Mathematics of Information Technology and Complex Systems (to EJV) and grant no. F3210-N18 of the Austrian Science Fund FWF (to GP).

## References

1. Li HG, Jones DL, Yee R. Defibrillation shocks produce different effects on Purkinje fibers and ventricular muscle: implications for successful defibrillation, refibrillation and postshock arrhythmia. J Am Coll Cardiol. 1993; 22:607–614. [PubMed: 8335836]
2. Berenfeld O, Jalife J. Purkinje-muscle reentry as a mechanism of polymorphic ventricular arrhythmias in a 3-dimensional model of the ventricles. Circ Res. 1998; 82:1063–1077. [PubMed: 9622159]

3. Cha YM, Birgersdotter-Green U, Wolf PL, et al. The mechanism of termination of reentrant activity in ventricular fibrillation. Circ Res. 1994; 74:495–506. [PubMed: 8118958]
4. Al-Khadra A, Nikolski V, Efimov I. The role of electroporation in defibrillation. Circ Res. 2000; 87:797–804. [PubMed: 11055984]
5. Pak HN, Oh Y, Liu Y, et al. Catheter ablation of ventricular fibrillation in rabbit ventricles treated with β-blockers. Circulation. 2003; 108:3149–3156. [PubMed: 14656917]
6. Tabereaux PB, Walcott G, Rogers JM, et al. Activation patterns of Purkinje fibers during long-duration ventricular fibrillation in an isolated canine heart model. Circulation. 2007; 116:1113–1119. [PubMed: 17698730]
7. Kim YH, Xie F, Yashima M, et al. Role of papillary muscle in the generation and maintenance of reentry during ventricular tachycardia and fibrillation in isolated swine right ventricle. Circulation. 1999; 100:1450–1459. [PubMed: 10500048]
8. Valderrbano M, Lee M, Ohara T, et al. Dynamics of intramural and transmural reentry during ventricular fibrillation in isolated swine ventricles. Circ Res. 2001; 88:839–848. [PubMed: 11325877]
9. Dosdall DJ, Tabereaux PB, Kim JJ, et al. Chemical ablation of the Purkinje system causes early termination and activation rate slowing of long-duration ventricular fibrillation in dogs. Am J Physiol Heart Circ Physiol. 2008; 295:H883–889. [PubMed: 18586887]
10. Salama G, Kanai A, Efimov I. Subthreshold stimulation of Purkinje fibers interrupts ventricular tachycardia in intact hearts: experimental study with voltage-sensitive dyes and imaging techniques. Circ Res. 1994; 74:604–619. [PubMed: 8137497]
11. Vigmond EJ, Weber Dos Santos R, Prassl AJ, et al. Solvers for the cardiac bidomain equations. Prog Biophys Mol Biol. 2008; 96:3–18. [PubMed: 17900668]
12. Mahajan A, Shiferaw Y, Sato D, et al. A rabbit ventricular action potential model replicating cardiac dynamics at rapid heart rates. Biophys J. 2008; 94:392–410. [PubMed: 18160660]
13. DeBruin K, Krassowska W. Modeling electroporation in a single cell. I. effects of field strength and rest potential. Biophys J. 1999; 77:1213–1224. [PubMed: 10465736]
14. Ashihara T, Trayanova N. Asymmetry in membrane responses to electric shocks: insights from bidomain simulations. Biophys J. 2004; 87:2271–2282. [PubMed: 15454429]
15. Vetter F, McCulloch A. Three-dimensional analysis of regional cardiac function: a model of rabbit ventricular anatomy. Prog Biophys Mol Biol. 1998; 69:157–183. [PubMed: 9785937]
16. Vigmond EJ, Clements C. Construction of a computer model to investigate sawtooth effects in the Purkinje system. IEEE Trans Biomed Eng. 2007; 54:389–399. [PubMed: 17355050]
17. Tranum-Jensen J, Wilde A, Vermeulen J. Morphology of electrophysiologically identified junctions between purkinje fibers and ventricular muscle in rabbit and pig hearts. Circ Res. 1991; 69:429–437. [PubMed: 1860183]
18. DiFrancesco D, Noble D. A model of cardiac electrical activity incorporating ionic pumps and concentration changes. Philos Trans Roy Soc Lond B Biol Sci. 1985; 307:353–398. [PubMed: 2578676]
19. Ramanathan C, Jia P, Ghanem R, et al. Activation and repolarization of the normal human heart under complete physiological conditions. Proc Natl Acad Sci USA. 2006; 103:6309–6314. [PubMed: 16606830]
20. Wiedmann RT, Tan RC, Joyner RW. Discontinuous conduction at Purkinje-ventricular muscle junction. Am J Physiol. 1996; 271:H1507–H1516. [PubMed: 8897946]
21. Efimov IR, Aguel F, Cheng Y, et al. Virtual electrode polarization in the far field: implications for external defibrillation. Am J Physiol Heart Circ Physiol. 2000; 279:H1055–H1070. [PubMed: 10993768]
22. Hillebrenner MG, Eason JC, Campbell CA. Postshock arrhythmogenesis in a slice of the canine heart. J Cardiovasc Electrophysiol. 2003; 14:S249–S256. [PubMed: 14760930]
23. Chattipakorn N, Fotuhi PC, Chattipakorn SC. Three-dimensional mapping of earliest activation after near-threshold ventricular defibrillation shocks. J Cardiovasc Electrophysiol. 2003; 14:65–69. [PubMed: 12625612]

24. Chen PS, Shibata N, Dixon EG, et al. Activation during ventricular defibrillation in open-chest dogs. evidence of complete cessation and regeneration of ventricular fibrillation after unsuccessful shocks. J Clin Invest. 1986; 77:810–823. [PubMed: 3949979]

25. Dosdall DJ, Cheng KA, Huang J, et al. Transmural and endocardial Purkinje activation in pigs before local myocardial activation after defibrillation shocks. Heart Rhythm. 2007; 4:758–765. [PubMed: 17556199]

26. Jalife J. Ventricular fibrillation: mechanisms of initiation and maintenance. Ann Rev Physiol. 2000; 62:25–52. [PubMed: 10845083]

27. Ashihara T, Constantino J, Trayanova NA. Tunnel propagation of postshock activations as a hypothesis for fibrillation induction and isoelectric window. Circ Res. 2008; 102:737–745. [PubMed: 18218982]

28. Huelsing D, Spitzer K, Cordeiro J. Conduction between isolated rabbit Purkinje and ventricular myocytes coupled by a variable resistance. Am J Physiol. 1998; 274:H1163–H1173. [PubMed: 9575919]

29. Wieser L, Nowak CN, Tilg B. Mother rotor anchoring in branching tissue with heterogeneous membrane properties. Biomed Tech Berl. 2008; 53:25–35. [PubMed: 18251708]

30. Tang L, Hwang GS, Song J, et al. Post-shock synchronized pacing in isolated rabbit left ventricle: evaluation of a novel defibrillation strategy. J Cardiovasc Electrophysiol. 2007; 18:740–749. [PubMed: 17388914]

31. Cerrone M, Noujaim SF, Tolkacheva EG, et al. Arrhythmogenic mechanisms in a mouse model of catecholaminergic polymorphic ventricular tachycardia. Circ Res. 2007; 101:1039–1048. [PubMed: 17872467]

Europe PMC Funders Author Manuscripts

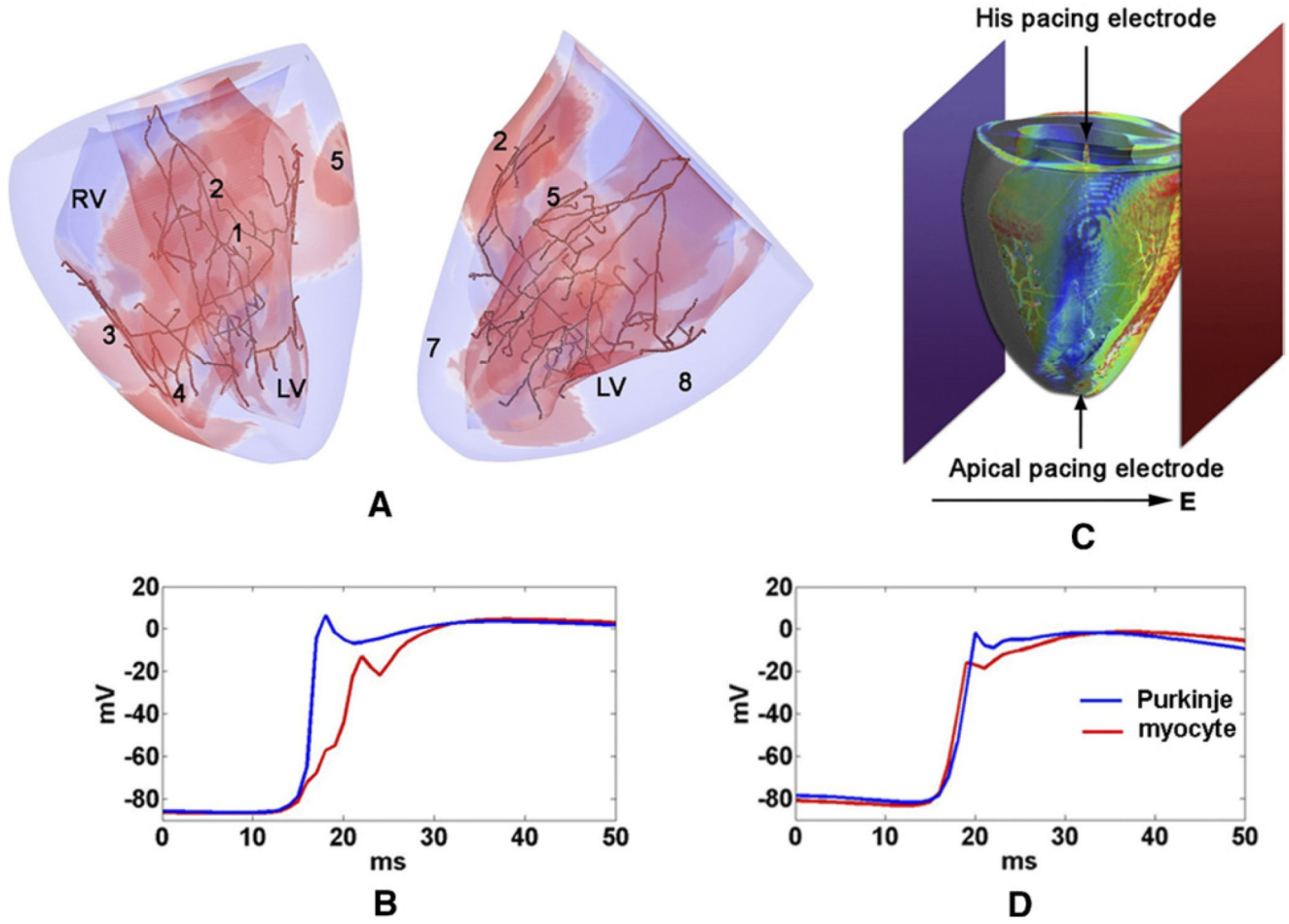


**Figure 1.**

Ventricular model with PS. **A:** Sinus activation 45 ms after His stimulation. Epicardial breakthrough sites are enumerated in order of occurrence. *Red regions* represent Vm >15 mV. **B:** Planar shocking electrodes are indicated at bath boundaries in *dark blue* and *red*. The electric field direction for cross shocks and the single-site pacing locations are indicated by arrows. **C, D:** Typical junctional propagation delays for anterograde and retrograde propagation, respectively.




Europe PMC Funders Author Manuscripts

Europe PMC Funders Author Manuscripts

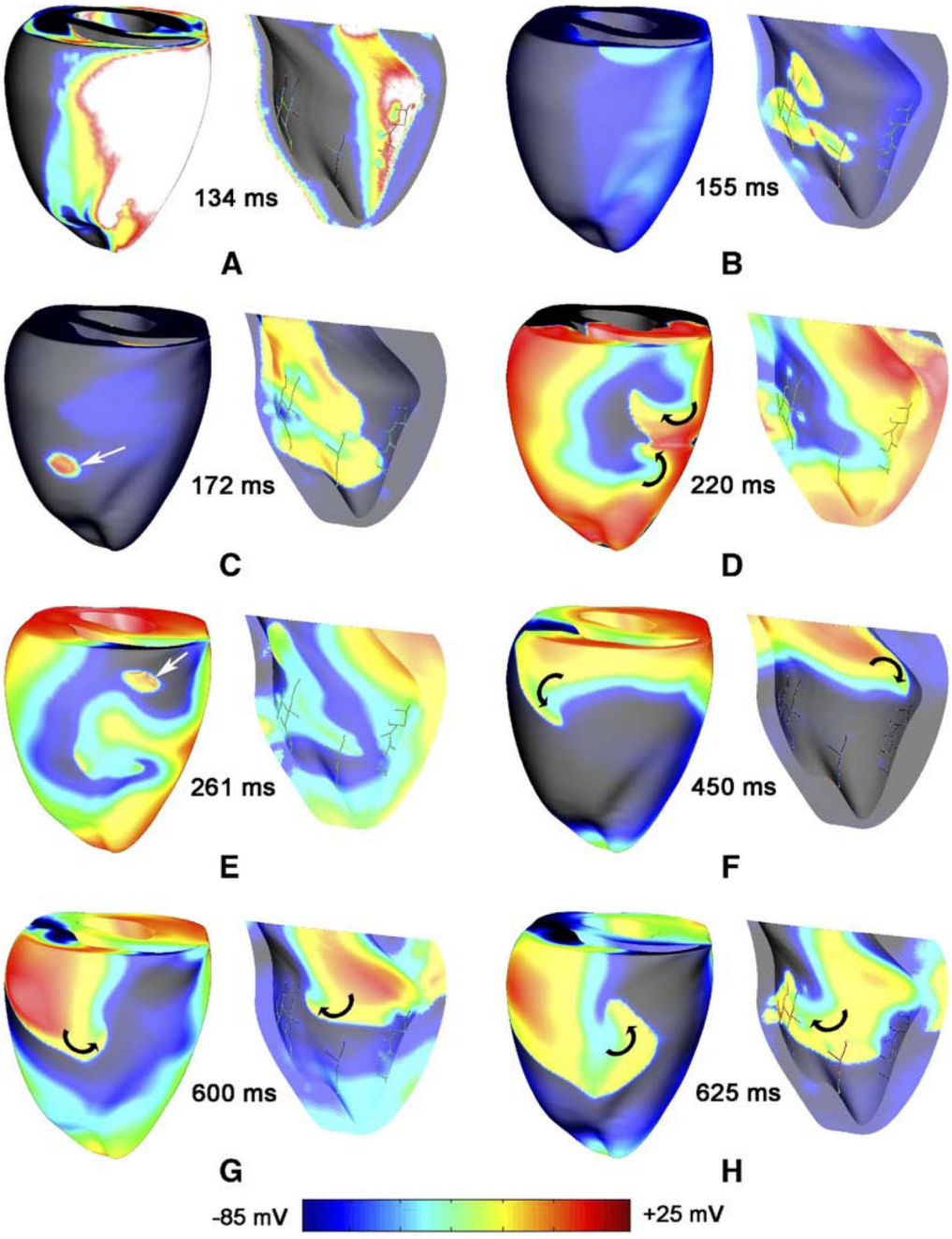


**Figure 2.**

Different stages in a typical reentry induced by burst pacing (BCL 130 ms, shock strength 3.6 V/cm). RV epicardium and LV endocardium are shown for each time instance. *White arrows* show epicardial breakthroughs from the PS. *Black arrows* indicate visible rotor paths. Vm is indicated by surface color.

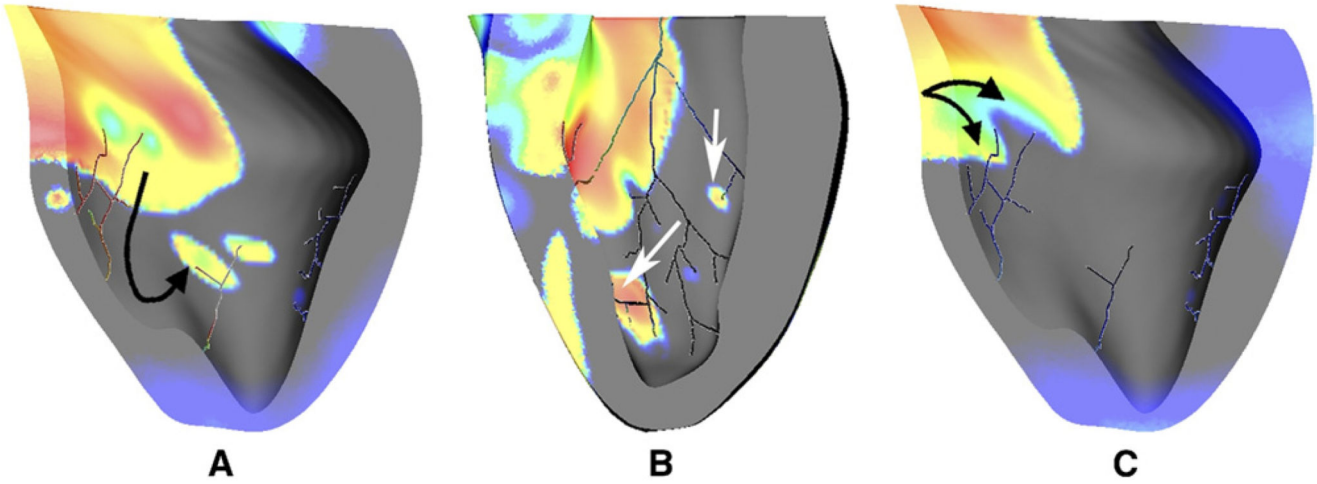


**Figure 3.**

PS contributions during reentry. **A:** The PS leads to wave front acceleration as activity enters the distal PS, propagates rapidly to distant unexcited myocardium (*black arrow*), and creates new wave fronts by anterograde propagation, which then merge with slower propagating myocardial activity. **B:** The PS provides escape routes (*white arrows*) for activity that would otherwise be extinguished. **C:** Refractory PS endpoints lead to wave front fractionation (*black arrows*). Vm is indicated by surface color, as in Figure 2.



Europe PMC Funders Author Manuscripts

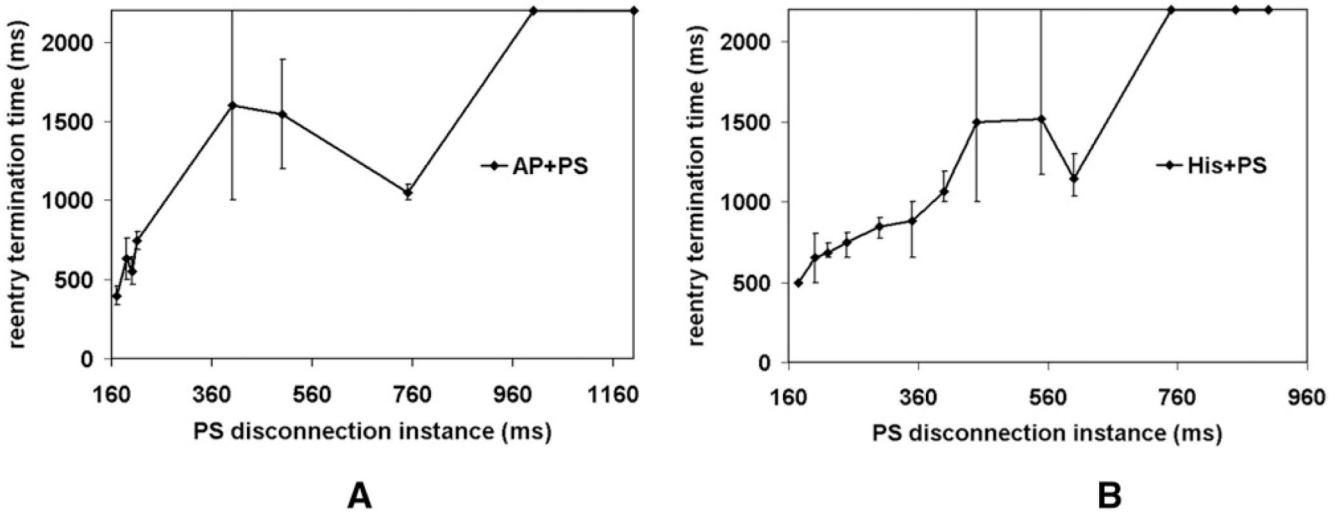


**Figure 4.**

Outcome after PS disconnection at various instances during reentry induced by AP+PS (panel A) and His+PS (panel B). Error bars indicate maximum deviation. In both cases, n = 3.





Europe PMC Funders Author Manuscripts

Europe PMC Funders Author Manuscripts

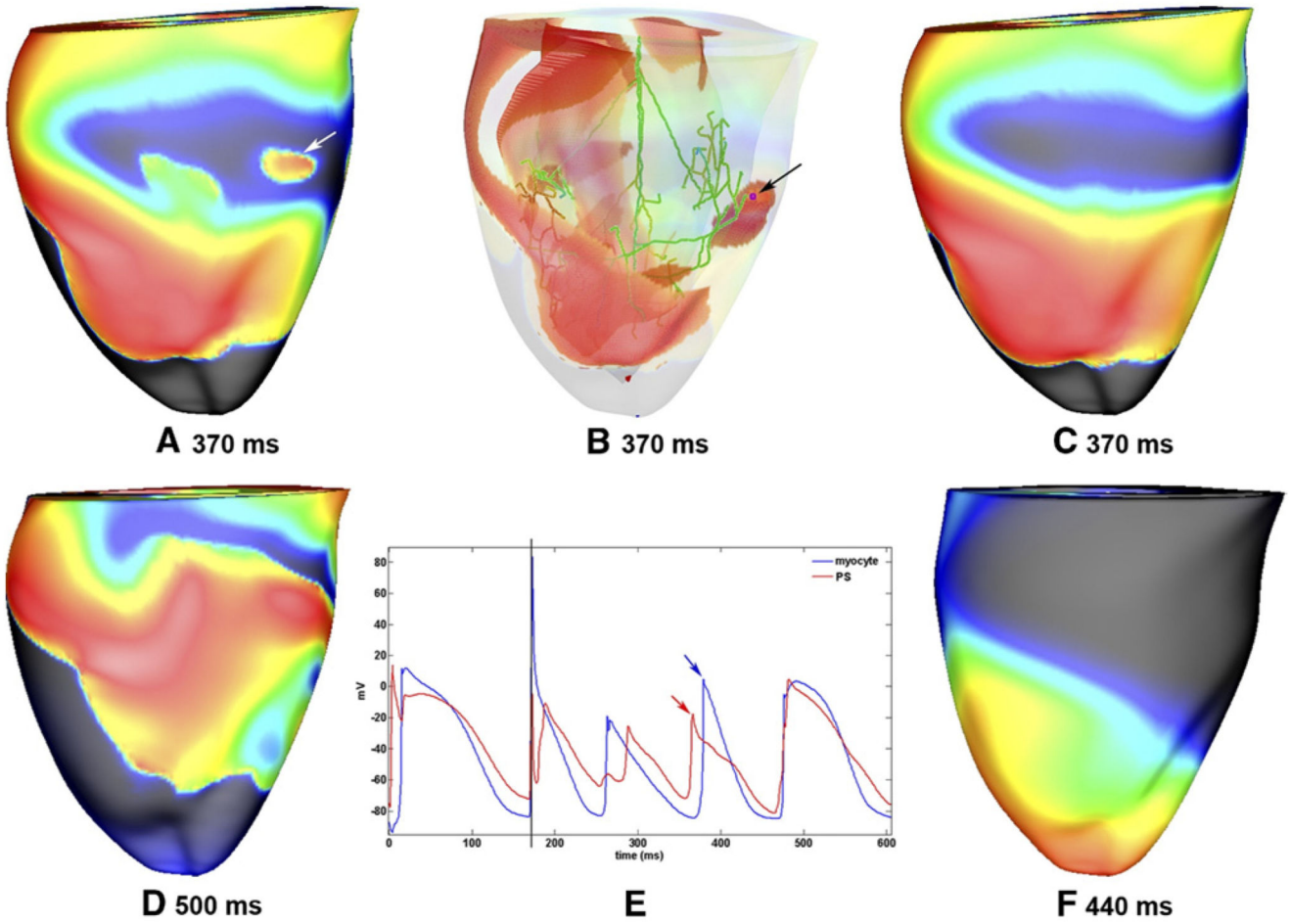


**Figure 5.**

Breakthrough provided by PS establishes reentry. **A:** Epicardial breakthrough (indicated by *white arrow*) during reentry initiated by AP+PS. **B:** The origin of the breakthrough highlighted in panel A is visible in the PS (indicated by *black arrow*). The corresponding PMJ is marked with a *pink dot*. *Red regions* represent Vm >15 mV. **C:** Same snapshot as in panel A but with the PS disconnected from the myocardium 200 ms after the initiation of reentry. The epicardial breakthrough seen in panel A is absent. After the snapshot in panel A, reentry continued, as shown in panel D; in contrast, after the snapshot in panel C, reentry was extinguished as a consequence of PS disconnection, as shown in panel F. **E:** Vm traces from the PS cell highlighted in panel B and an epicardial myocyte at the breakthrough site highlighted in panel A. Action potentials corresponding to the breakthrough are indicated by *arrows*, and the 4 V/cm cross shock applied at a CI of 170 ms is indicated by a *vertical line*. Except in panels B and E, Vm is indicated by surface color, as in Figure 2.

Europe PMC Funders Author Manuscripts

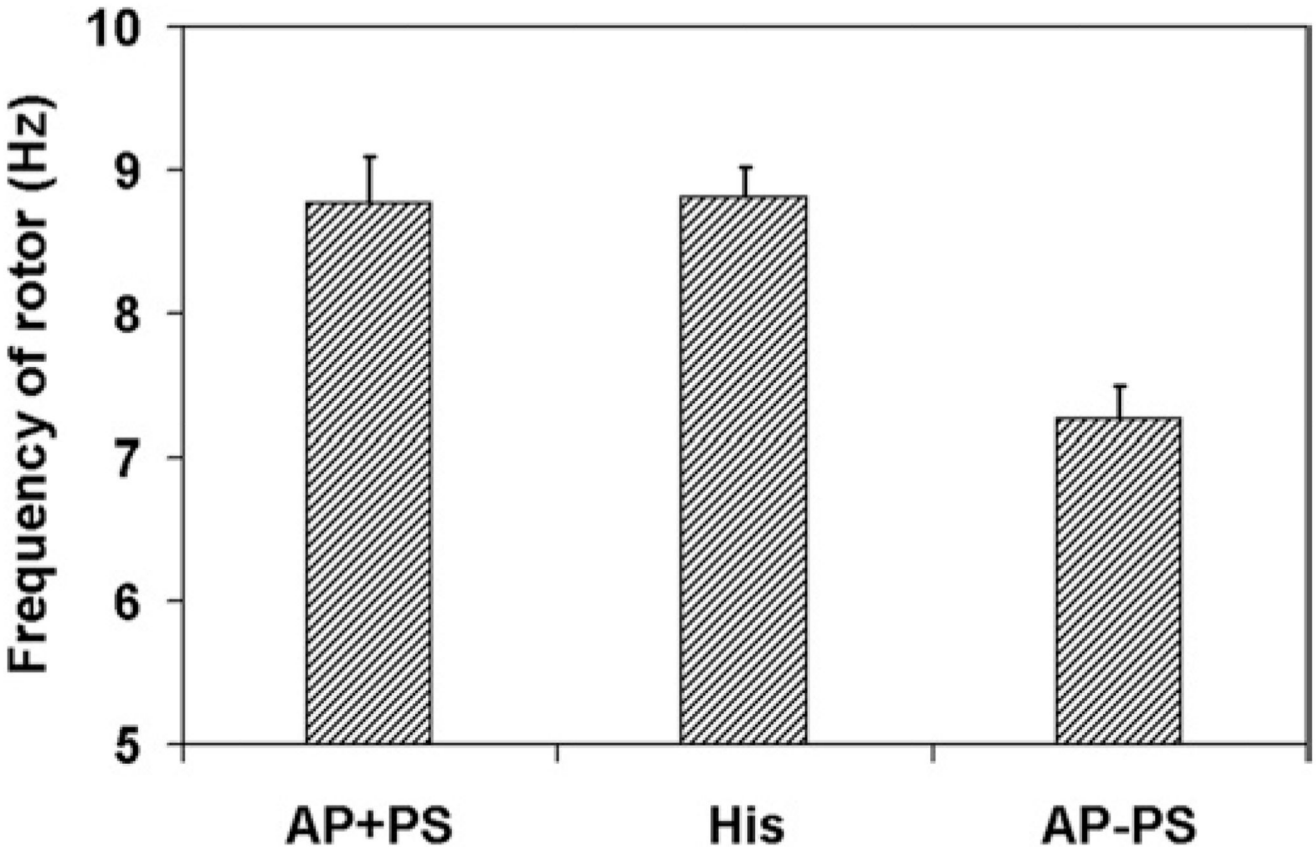


**Figure 6.**

Rotor frequency in later stages of reentry for AP+PS, His, and AP−PS. Error bars indicate maximum deviation. In all cases, n = 3.

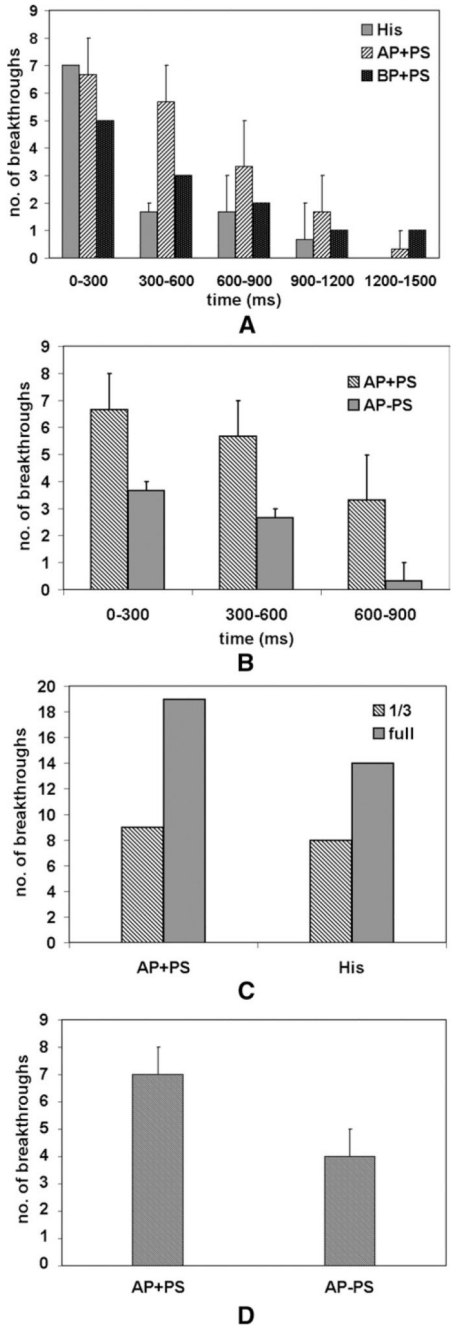


**Figure 7.**

The number of breakthroughs observed decreased during reentry. **A:** Breakthroughs over time for different reentry induction protocols with PS. His: CI 165 ms; AP+PS: CI 150 ms; shock strengths: 4.3, 4.7, and 5 V/cm. BP+PS: BCL 130 ms; shock strengths: 3.3, 4, and 4.3 V/cm. **B:** Breakthroughs over time for simulations with and without the PS. **C:** Early-stage breakthroughs (0–600 ms) for different PS penetration depths (one-third, as in the rest of this study, compared with full-wall penetration, with endpoints located subepicardially). **D:**

Breakthroughs observed after failed 4 V/cm defibrillation shocks (0–400 ms) with22 and without the PS. Error bars indicate maximum deviation. In all cases except panel C, n = 3.



Europe PMC Funders Author Manuscripts

Europe PMC Funders Author Manuscripts

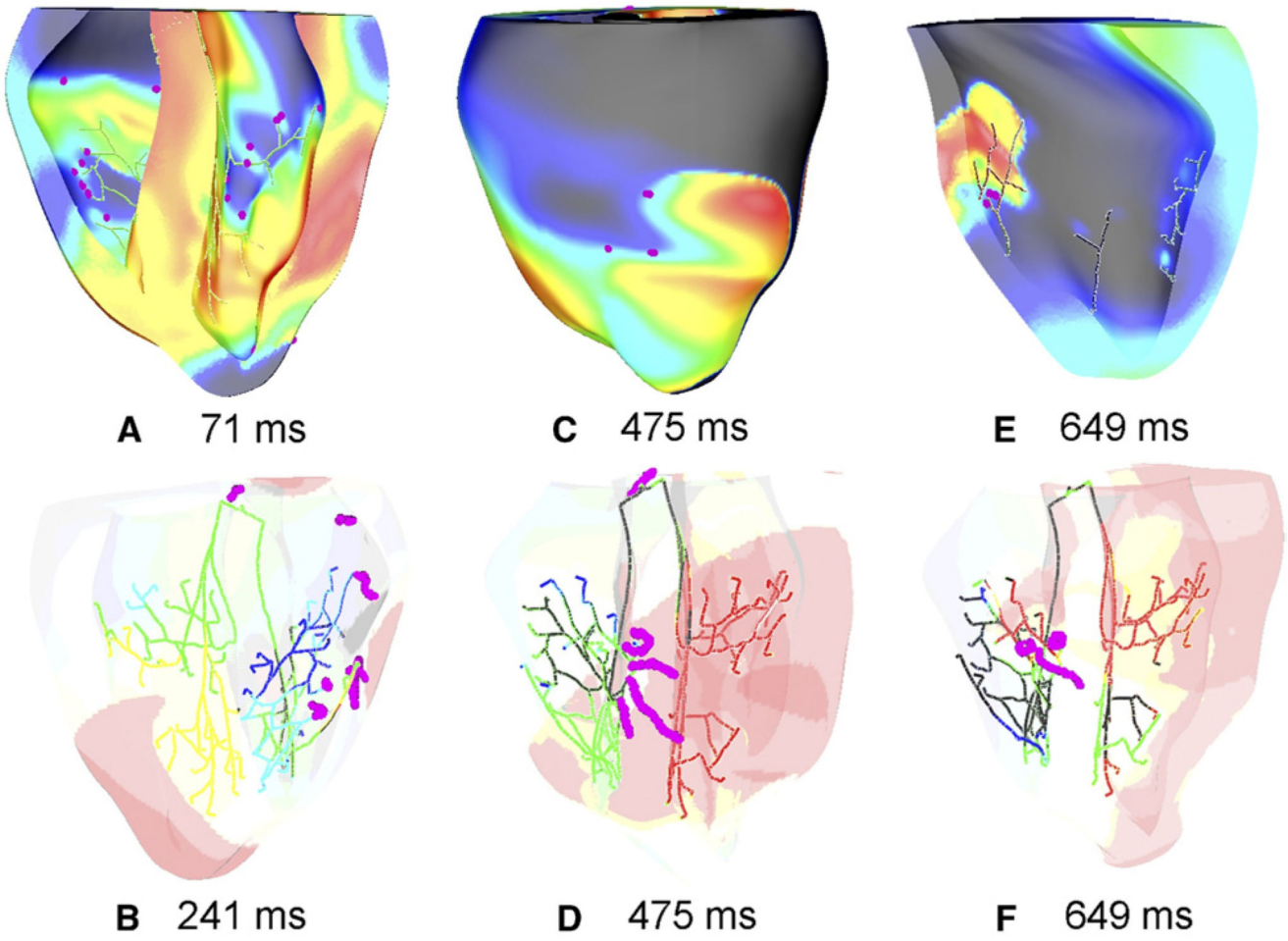


**Figure 8.**

Phase analysis at various instants during reentry. Phase singularities (*pink dots*) were concentrated around the distal PS network. Reentrant filaments were consistently anchored to PS endpoints as seen in panels B, D, and F. *Upper panels*: Vm is indicated by surface color, as in Figure 2. *Lower panels*: *red regions* represent Vm >15 mV.

Europe PMC Funders Author Manuscripts

**Table 1**

Reentry inducibility for different protocols

| | Reentry protocols | | | | |
|---|---|---|---|---|---|
| | **AP+PS** | **AP−PS** | **BP+PS** | **BP−PS** | **His** |
| Minimum shock strength, V/cm | 3.3 | 4.0 | 3.6 | 6.0 | 3.3 |
| CI/BCL range, ms | 145–155 | 145–160 | 125–135 | 125–135 | 165–175 |